

HEALNet - Hybrid Multi-Modal Fusion for Heterogeneous Biomedical Data

Konstantin Hemker¹, Nikola Simidjievski^{1,2}, Mateja Jamnik¹

¹ Department of Computer Science & Technology

² Department of Oncology

University of Cambridge

{kh701, ns779, mj201}@cam.ac.uk

Abstract

Technological advances in medical data collection such as high-resolution histopathology and high-throughput genomic sequencing have contributed to the rising requirement for multi-modal biomedical modelling, specifically for image, tabular, and graph data. Most multi-modal deep learning approaches are using modality-specific architectures that are trained separately and cannot capture the crucial cross-modal information that motivates the integration of different data sources. This paper presents the Hybrid Early-fusion Attention Learning Network (HEALNet) – a flexible multi-modal fusion architecture, which a) preserves modality-specific structural information, b) captures the cross-modal interactions and structural information in a shared latent space, c) can effectively handle missing modalities during training and inference, and d) enables intuitive model inspection by learning on the raw data input instead of opaque embeddings. We conduct multi-modal survival analysis on Whole Slide Images and Multi-omic data on four cancer cohorts of The Cancer Genome Atlas (TCGA). HEALNet achieves state-of-the-art performance, substantially improving over both uni-modal and recent multi-modal baselines, whilst being robust in scenarios with missing modalities.

Introduction

A key challenge in Multi-modal Machine Learning (MMML) is *multi-modal fusion*, which is the integration of heterogeneous data into a common representation that reduces the dimensionality of the data whilst preserving salient biological signals (Steyaert et al. 2023). Fusion approaches are well-studied in areas where there is a clearly defined shared semantic space, such as audio, visual, and text tasks such as visual question answering (Goyal et al. 2016), image captioning (Yu et al. 2020), or multi-modal dialogue (Liang, Zadeh, and Morency 2023). However, healthcare data commonly consists of 2D/3D images (histopathology and radiology), graphs (molecular data), and tabular data (multi-omics, EHRs) where cross-modal relationships are typically more opaque and complex, and common representations less explored. The *fusion stage* describes how far the multi-modal representation is removed from the raw (uni-modal) data and is commonly categorised into

early, intermediate, and late fusion (Baltrusaitis, Ahuja, and Morency 2019). Early fusion approaches combine the raw data early in the pipeline, which allows training a single model from all data modalities simultaneously. However, most of these approaches use simple operations such as concatenation, which removes structural information, or take the Kronecker product (Chen et al. 2022a), which can lead to exploding dimensions when applied to multiple modalities and large matrices. Late fusion, on the other hand, trains separate models for each modality at hand, which allows capturing the salient structural information but prevents the model from learning interactions between modalities (Liang, Zadeh, and Morency 2023). Intermediate fusion approaches attempt to overcome this trade-off by learning a low-level representation (embedding) for each modality before combining them. This can result in discovering the cross-modal interactions whilst taking advantage of each modality’s internal data structure. The problem with many intermediate fusion approaches is that the learnt latent representation is not interpretable to human experts, and handling missing modalities is often noisy (Cui et al. 2023). To overcome these issues, we posit that there is a need for more sophisticated early fusion methods, which we refer to as *hybrid early fusion*, that a) preserve structural information and learn cross-modal interactions b) learn cross-modal interactions, and c) work on the raw data, thus allowing for in-model explainability.

In this paper, we propose **Hybrid Early-fusion Attention Learning Network** (HEALNet, Figure 1), a novel *hybrid early fusion* approach that leverages the benefits of early and intermediate fusion approaches. The main idea behind HEALNet is to use both a shared and modality-specific parameter space in parallel within an iterative attention architecture. Specifically, a shared latent bottleneck array is passed through the network and iteratively updated, thus capturing shared information and learning tacit interactions between the data modalities. Meanwhile, attention weights are learned for each modality and are shared between layers to learn modality-specific structural information. We demonstrate the multi-modal utility of HEALNet on survival analysis tasks on four cancer sites from The Cancer Genome Atlas (TCGA) data, combining multi-omic (tabular) and histopathology slides (imaging) data. Our results show that HEALNet achieves state-of-the-art concordance

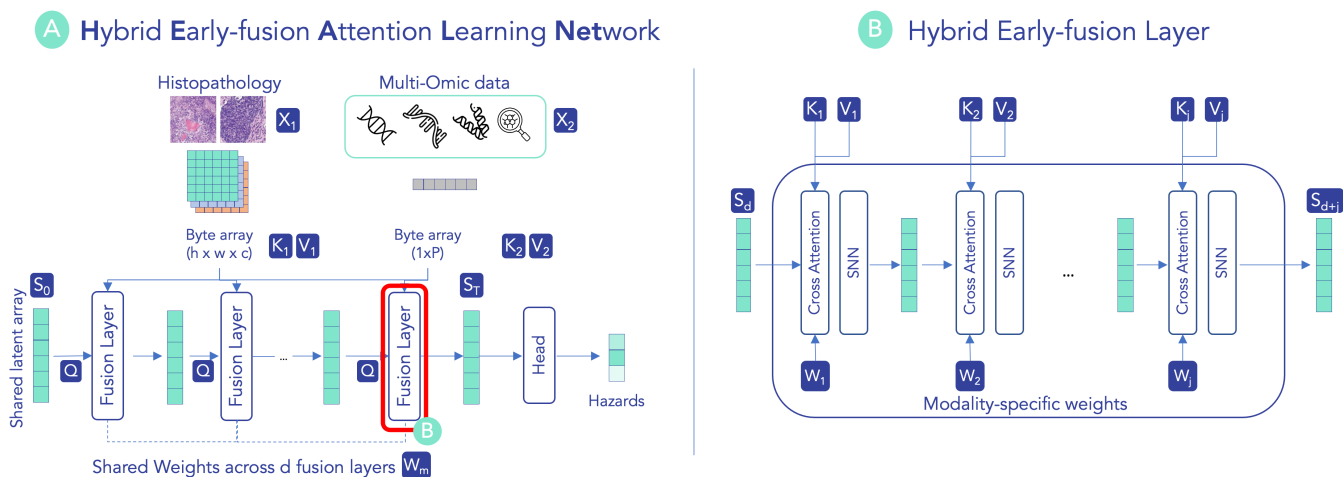


Figure 1: Overview of HEALNet (**H**ybrid **E**arly-fusion **A**ttention **L**earning **N**etwork) using a shared *and* modality-specific parameter space to learn from structurally heterogeneous data sources in the same model (Fig. 1A). The shared space is a query array S that is iteratively updated through d attention-based fusion layers, and captures the shared information between modalities. The hybrid early fusion layer (Fig. 1B, and Eq. 3) learns the attention weights $W_m = \{W_m^{(q)}, W_m^{(k)}, W_m^{(v)}\}$ for each modality m corresponding to the queries ($Q_m = W_m^{(q)} S$), keys ($K_m = W_m^{(k)} X_m$), and values ($V_m = W_m^{(v)} X_m$) which are shared between layers. These layers capture structural information of each modality before encoding them in the shared array.

Index (c-Index) performance on all four cancer datasets for multi-modal patient survival prediction. More specifically, HEALNet leads to an average improvement of up to 7% compared to the best uni-modal benchmarks and up to 4.5% compared to the best early, intermediate, and late fusion benchmarks, which we see as a promising validation of our hybrid early fusion paradigm. In summary, the contributions of our proposed HEALNet include:

- Preserving the modality-specific structure: Despite no modality-specific network topology, HEALNet outperforms uni-modal tabular (omic) and imaging (histopathology) baselines.
- Learning cross-modal interactions: HEALNet effectively captures cross-modal information, achieving a significantly higher multi-modal uplift compared to existing early, intermediate, and late fusion baselines.
- Handling missing modalities: We show that HEALNet effectively handles missing modalities at inference time without introducing further noise to the model, a common problem in the clinical use of multi-modal models.
- Easy inspection: HEALNet is explainable ‘by design’, since the modality-specific attention weights can provide insights about what the model has learned without the need for a separate explanation method. While we are yet to validate these explanations for clinical relevance, we believe that they are useful for model debugging.

Related Work

In this paper, we focus on multi-modal learning problems from biomedical data, where the data modalities are *structurally heterogeneous*, specifically combining image (e.g., Whole Slide Imagery (WSI)) and tabular (e.g., omic and

clinical) data. This aspect is different and more general than approaches that focus on combining homogeneous modalities, such as multi-omic data, where the combined modalities have the same structural formalism (tabular) (Sammur et al. 2021; Dai, Gao, and Liu 2021). As such, our work closely relates to several approaches for multi-modal data fusion that consider learning from WSI images and genomic data. Namely, (Cheerla and Gevaert 2019) introduce a two-step procedure, combining a self-supervised pre-training step with a downstream fine-tuning for survival analysis. In the first self-supervised step, a modality-specific embedding is trained and optimised using a similarity loss (similar to contrastive learning) between the embeddings. The latter step includes (supervised) fine-tuning of a survival model, trained and optimised using the Cox loss. HEALNet, on the other hand, implements end-to-end training with an additive approach to combining modalities (rather than handling them in parallel). As such, it can scale and generalise well on problems from data with different sizes and properties without requiring explicit pre-training. Nevertheless, the design of HEALNet allows for leveraging pre-trained model encoders, which may further improve its performance on a particular task of interest.

HEALNet capabilities for multi-modal fusion build on attention architectures (Vaswani et al. 2017). In this context, it also relates to approaches implementing a cross-modal attention component for intermediate and/or late fusion. ‘Multi-modal co-attention’ (MCAT) (Chen et al. 2021) is an attention-based fusion approach that uses the tabular modality as the query and the imaging modality as the key and value array to train a cross-attention unit. This unit further serves as the main encoder ahead of the downstream task. Note that the co-attention only scales to two modalities since

such co-attention units can only take in one set of query-key-value inputs. Chen et al. (2022a) present an intermediate fusion approach that first constructs modality-specific embeddings before passing them through a gating-based attention mechanism, combining the output via a Kronecker product. In turn, the resulting high-dimensional ‘3D multi-modal tensor’ is used for a downstream survival prediction task. Similarly, Chen et al. (2022b) propose ‘Porpoise’, a late fusion approach which implements modality-specific model encoders before combining each model’s output via a gating mechanism. In the case of ‘Porpoise’, the attention mechanism is only applied to the imaging modality (WSI), which serves as a method for learning more general representations by combining the patch-level latents, but also allows for explainable post-hoc image analysis of the identified regions. As such, an inherent limitation of such an approach is that it only applies to and considers uni-modal explanations.

In contrast, HEALNet overcomes many of the limitations of the related fusion approaches. First, its design readily scales to more than two modalities without additional computational overhead beyond the one introduced by the additional modality-specific encoders. Namely, the iterative attention mechanism alleviates the use of fusing operators (such as a Kronecker product) that render high-dimensional embeddings and allows for combining many modalities while preserving the structural information of each. Moreover, since HEALNet is an early fusion approach, it is able to learn cross-modal interactions whilst working directly on the raw input data. More importantly, this allows for better and holistic explainable capabilities, which is not the case for the late fusion approaches that use modality-specific models trained in isolation.

HEALNet

Preliminaries. Let X_m represent data from modality $m = 1, \dots, j \in \mathbb{N}$. Let $X_m \in \mathbb{R}^{p \times n}$ be either a tabular dataset with p features and n samples; or an image dataset $X_m \in \mathbb{R}^{h \times w \times c \times n}$ with n images with height h , width w and channels c . The goal of a multi-modal fusion approach is to learn a fusion function $f()$ such that $y = f(X_1, \dots, X_j; \theta)$ where θ denotes the set of hyperparameters. A conventional design of such a system (such as the related work discussed previously) is to first learn a modality-specific function $g_m()$ which learns an intermediate representation $h_m = g_m(X_m; \phi_m)$ for intermediate hyperparameters ϕ and then apply a fusion function $f()$ for predicting the target variable $\hat{y} = f(h_1, \dots, h_j; \theta)$.

Architecture. We depict HEALNet in Figure 1. Instead of computing h_m and applying a single fusion function $f()$, HEALNet uses an iterative learning setup. Let t denote a step, where the total number of steps $T = d \times m$ for the number of fusion layers $d \in \theta$. Let S_t represent a latent array shared across modalities, initialised at S_0 where $S \in \mathbb{R}^{a \times b}$ and $a, b \in \phi$ which is updated at each step. First, instead of learning an intermediate representation h_m as encoded inputs for X_m , we compute the attention weights as

$$a_m^{(t)} = \alpha(X_m, S_t; \phi^{a_m}), \quad (1)$$

for each modality m at each step t . Second, we learn an update function $\psi()$ to be applied at each step. The update of S with modality m is given by

$$S_{t+1,m} = \psi(S_t, a_m^{(t)}; \rho), \quad (2)$$

where ρ denotes the shared hyperparameters across T . For parameter efficiency, the final implementation uses weight sharing between layers. Across modalities, each early-fusion layer becomes an update function of the form

$$S_{t+j} = \psi(S_t, a_1, \dots, a_j; \rho). \quad (3)$$

The final function for generating a prediction only takes the final state of the shared array and returns the predictions of the target variable $\hat{y} = f(S_T; \theta)$.

Figure 1 depicts a high-level visual representation of this approach, showing (a) Hybrid Early-fusion Attention Learning Network and (b) its key component, the early fusion layer (as given in Equation 3). We structure the early fusion model as an attention network due to its ability to be generally applicable in different settings, making fewer assumptions about the input data (e.g., compared to a convolutional network). We start by randomly initialising a latent bottleneck array, which is iteratively used as a query into each of the fusion layers and is updated with information from the different modalities at each layer pass. The iterative attention paradigm is inspired by the Perceiver model (Jaegle et al. 2021), which we chose due to its highly competitive performance on a range of uni-modal tasks. Passing the modalities through the shared latent array helps to significantly reduce the dimensionality whilst learning important structural information through the cross-attention layers. The HEALNet pseudocode is detailed further in Appendix A.

Preserving structural information. To handle heterogeneous modalities, we use modality-specific cross-attention layers $\alpha()$ and their associated attention weights $a_m^{(t)}$, whilst having the latent array S shared between all modalities. Sharing the latent array between modalities allows the model to learn from information across modalities, which is repeatedly passed through the model (Fig. 1A). Meanwhile, the modality-specific weights between of the cross-attention layers (Fig. 1B) focus on learning from inputs of different dimensions as well as learning the implicit structural assumptions of each modality. Specifically, in this work, the employed attention mechanism refers to the original scaled dot product attention from (Vaswani et al. 2017), with adjustments for tabular and image data.

Formally, given tabular dataset as a matrix $X_m = \{x_m^{(11)}, \dots, x_m^{(np)}\}$, with $n \in N$ samples and $p \in P$ features (e.g., a gene expression), we aim to learn the weight matrices $W_m^{(q)}$, $W_m^{(k)}$, and $W_m^{(v)}$ that act as a linear transformation for S and X_m that form the queries ($q_m^{(n)}$), keys ($k_m^{(n)}$) and values ($v_m^{(n)}$) for each sample passed into the layer. The general scale dot-product attention generates attention scores for each feature and can be expressed in Cartesian Notation as

$$A_p(q_p, K) = \sum_{i=1}^P \left[\frac{\exp(q_p \cdot k_i^P)}{\sum_j \exp(q_p \cdot k_j^P)} \right] \quad \forall j \in [1, N]. \quad (4)$$

In other words, for each channel p and sample n , an attention layer calculates the normalised and scaled attention weight being given the context of all other features for that sample. This has the benefit that the attention scores are always specific to each input given to the attention layer. From this, we can extract both the normalised attention matrix A as well as the context matrix $C_p(q, K, V) = \sum_{i=1}^P A_{p,i} \times v_i$, which is the attention-weighted version of the original input x . In our case, we need to combine multiple inputs to apply the iterative attention mechanism (i.e., cross-attention) – these inputs are the latent S and the input matrix X_m for each modality. To do this, we use the latent array as the query and the input tensor as the keys and values, respectively. Given a latent array S , we define the query for each sample $q_m^{(n)} = W_m^{(q)} S$ and the keys and values as $k_m^{(k)} = W_m^{(k)} x^{(n)}$ and $v_m^{(n)} = W_m^{(v)} x^{(n)}$ for all $n \in [1, N]$.

High-dimensional biomedical data. Attention-based architectures are typically trained on extremely large datasets (which are commonly available for vision and language tasks). The challenges of working with biomedical data, however, are their high dimensionality whilst often having relatively few samples (i.e., patients). For example, a dataset (such as TCGA-BLCA) can have a whole slide image of approximately 6,4 gigapixels ($80k \times 80k$ pixels) in its highest resolution, includes thousands of multi-omic features, but only contains a few hundred patients in total. This leads to two common problems in digital pathology – overfitting and high computational complexity. First, to counteract overfitting, HEALNet implements both L1 and L2 regularisation. Considering the relatively large number of parameters required for the attention layers, we found L1 regularisation to be important. Beyond that, we opted for a self-normalising neural network (SNN) block, due to its proven robustness and regularisation properties (Klambauer et al. 2017).

Second, handling the extremely high resolution of the whole slide images (WSIs) within computational constraints is also a challenge. We address this by extracting non-overlapping 256x256 pixel patches on the 4x downsampled whole-slide image. For comparability with other work, we extract a 2048-dimensional feature vector for each patch using a standard ResNet50 pre-trained on ImageNet-1k v2 (Krizhevsky, Sutskever, and Hinton 2012). While HEALNet also achieves similar results on the raw patch data, this requires more significant downsampling in order to be computationally feasible. For this reason, in this study, we only ran the raw image data on a single cancer site (BLCA) and used the patch feature encodings for the full experiment runs.

Handling missing modalities. Another common challenge in clinical practice is missing data modalities during inference. Namely, in practical scenarios, while models have been trained on multiple modalities, there is a great chance that not all data modalities are available for predicting the patient’s outcome. Therefore, it is imperative that multi-modal approaches are robust in such scenarios. Typical intermediate fusion approaches would need to randomly initialise a tensor of the same shape, or sample the latent space for a semantically similar replacement to pass into the fusion function $f(h^1, \dots, h^j; \theta)$ at inference, which is likely to

introduce noise. In contrast, HEALNet overcomes this issue by design: the iterative paradigm can simply skip a modality update step (Equation 3) at inference time in a noise-free manner. Note that these practical benefits also extend to training scenarios, where a (typically small) number of samples are missing some modalities. Rather than imputing this data or completely omitting the samples, HEALNet is able to train and utilise all the available data using the same update principle.

Experiments

Datasets. We empirically evaluate the utility of HEALNet on survival analysis tasks from four cancer datasets from The Cancer Genome Atlas (TCGA). Concretely, we use modalities which are structurally heterogeneous such as the ones formalised in a tabular or image dataset. As such, our setup includes several tabular data sources (which are homogeneous) including gene expressions (whole-genome sequencing), mutations (RNAseq) and clinical variables - which in the continuation we refer to as the *omic modality*. Our WSI modality, includes H&E-stained whole slide tissue images of the same patient cohorts as in the omic modality. Namely, the four cancer datasets that we include are Muscle-Invasive Bladder Cancer (BLCA, n=436), Breast Invasive Carcinoma (BRCA, n=1021), Cervical Kidney Renal Papillary Cell Carcinoma (KIRP, n=284), and Uterine Corpus Endometrial Carcinoma (UCEC, n=538) (further dataset details are provided in Appendix C). These specific sites were chosen based on their sample size (BRCA, BLCA, and UCEC are some of the largest TCGA datasets), performance indicators reported in previous uni-modal studies (e.g., KIRP highest on omic, UCEC highest on WSI only (Chen et al. 2022b)), and other omic properties (e.g., BLCA and UCEC are known for their very high gene mutation rate (Ma, Laster, and Dong 2022)).

Task setup. For each patient, we are provided with right-censored censorship status c (a binary variable on whether the outcome was observed at the end of the study or not) and survival months since data recording. In line with our baselines (Chen et al. 2022b), we take non-overlapping quartiles k for the uncensored patients and apply them to the overall population, which assigns a categorical survival risk to each patient. For the survival task, our prediction model and the baselines are set to output logits of these survival buckets $y_{logits} = f(X_m, S; \theta, \rho)$. Using these, we calculate the hazard as the sigmoid of the logits $f_{hazard} = \frac{1}{1 + e^{-y_{logits}}}$, and the corresponding survival as $f_{survival} = \prod_1^k 1 - f_{hazard}$. The survival, hazards, censorship status and discretised survival label are all used to calculate the negative log-likelihood (NLL) loss from the proportional hazards model defined in (Zadeh and Schmid 2021). The concordance index is then calculated by comparing all study subject pairs to determine the fraction of pairs in which the predictions and outcomes are concordant (Brentnall and Cuzick 2018).

During development, we found that the proportion of uncensored patients sometimes can be as little as 15% of the cohort (UCEC). Applying the survival bins from such a small sub-sample lead to very imbalanced discretised sur-

Table 1: Mean and standard deviation of the concordance Index on four survival risk categories. We trained HEALNet and all baselines on four TCGA tasks and report the performance on the hold-out test set across five cross-validation folds. HEALNet outperforms all of its multi-modal baselines and three out of four uni-modal baselines in absolute c-Index performance.

Model	BLCA	BRCA	KIRP	UCEC
Uni-modal (Omics)	0.606 ± 0.019	0.580 ± 0.027	0.780 ± 0.035	0.550 ± 0.026
Uni-modal (WSI)	0.556 ± 0.039	0.550 ± 0.037	0.533 ± 0.099	0.630 ± 0.028
Porpoise	0.620 ± 0.048	0.630 ± 0.040	0.790 ± 0.041	0.590 ± 0.034
MCAT	0.620 ± 0.040	0.589 ± 0.073	0.789 ± 0.087	0.589 ± 0.062
Early Fusion	0.565 ± 0.042	0.566 ± 0.068	0.783 ± 0.135	0.623 ± 0.107
HEALNet (ours)	0.668 ± 0.036	0.638 ± 0.073	0.812 ± 0.055	0.626 ± 0.037

vival on the full cohort. To counteract this, we added the option to apply survival class weighting in the loss function, implemented as the inverse weight of the survival bins. Additionally, note that the NLL loss and the concordance index are sometimes only loosely related. Therefore, our loss weighting helped to stabilise the correlation between the NLL loss and the c-index. To ensure fair comparison and comparability with the baselines, we employed the same NLL loss and weighting for training HEALNet. Nevertheless, HEALNet is readily extensible and can be implemented with other survival loss functions such as the Cox loss, which can potentially lead to more stable c-Index results (Cheerla and Gevaert 2019).

Baselines. In all experiments, we compare HEALNet state-of-the-art uni- and multi-modal models that utilise different fusion strategies:

- **Porpoise** (Late Fusion): Uses a late fusion gating method to combine the latent representations h_m learned from a self-normalising network (SNN) on the omic features and an attention-based multiple-instance learning network (AMIL). Achieves the highest performance of late fusion models for pathology we came across (Chen et al. 2022b).
- **MCAT** (Intermediate Fusion): The Multi-modal Co-Attention Transformer (MCAT) uses two encoders as f_m – a “genomic-guided” co-attention followed by a set-based MIL Transformer. The resulting embeddings h_m are then concatenated and passed into a simple classifier (Chen et al. 2021).
- **Early Fusion**: For our early fusion baseline, we concatenate the whole slide image and omic input features into a single flattened tensor and pass it into HEALNet as a single modality.
- **WSI/Omic Only**: For each of our multi-modal baselines, we re-ran the uni-modal baselines reported in the respective papers as well as trained HEALNet on a single modality and report the best uni-modal model out of the set. The full results of all uni-modal baselines can be found in Appendix B.

Implementation details. For each experiment, we perform 5-fold cross-validation using a 70-15-15 train-test-validation split. All reported results show the models’ performance on test data that was not used during training or validation. We re-train all of the baseline models using the

code reported in the respective papers. All models have been run under the same circumstances and using the same evaluation framework (including data splits and loss weighting). For hyperparameter tuning, we ran a Bayesian Hyperparameter search (Bergstra, Yamins, and Cox 2013) using the same set of parameters for each dataset for all models. All final experiments were run on a single Nvidia A100 80GB GPU running on a Ubuntu 22.04 virtual machine. HEALNet is implemented in the PyTorch framework and available open-source at <https://github.com/konst-int-i/healnet>.

Results

The results of the survival analysis are summarised in Table 1, showing the mean and standard c-Index across the 5 cross-validation folds. Across all tested cancer sites, HEALNet outperforms all multi-modal baselines, achieving state-of-performance in three (out of four) cases. This corresponds to an improvement over the multi-modal baselines of approximately 7%, 1%, 3% and 6% on the BLCA, BRCA, KIRP, and UCEC tasks respectively. HEALNet also exhibits more stable behaviour compared to the multi-modal baselines, as evident from the standard deviation (across folds) which is lower in three out of four datasets.

The uni-modal baselines shown in Table 1 correspond to the best-performing models from a selection of uni-modal baselines we trained (refer to the complete list in Appendix B). Compared to the better of the two uni-modal baselines, HEALNet achieves an approximately 10% higher C-Index on BLCA and BRCA, a 4% higher c-Index on KIRP, and a nearly equivalent performance UCEC. We refer to this as *multi-modal uplift*, which is also illustrated in Figure 2, where we compare the improvement of the different multi-modal models and fusion strategies to the best uni-modal model. Note that the UCEC dataset is an example of *modality dominance*, where all informative signal stems from one modality (in this case WSI), while the other can be either non-informative or noisy. Intermediate and late fusion approaches, which directly combine modalities, are less robust in such cases. For instance, in the case of Porpoise and MCAT, this can even lead to performance degradation. Since HEALNet is more robust to such noise, it leads to comparable performance, compared to the uni-modal variant.

To further assess the robustness of HEALNet, we evaluate its performance in scenarios with missing modalities.

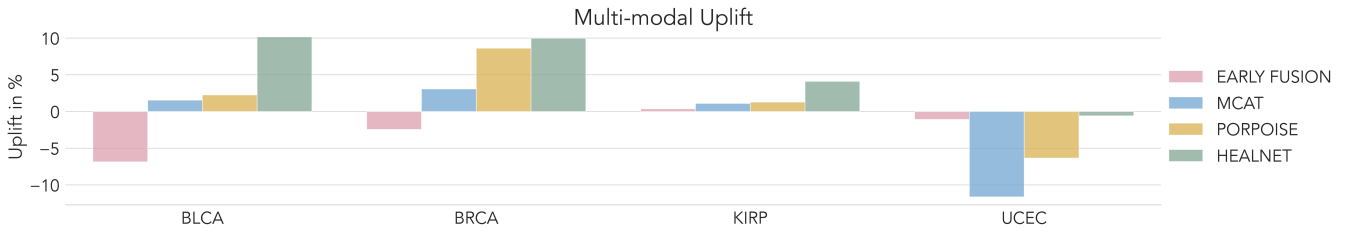


Figure 2: Mean percentage uplift of all multi-modal models compared to the best uni-modal baseline. Across all tested TCGA cancer sites, the *hybrid early fusion* paradigm that HEALNet uses outperforms early, intermediate, and late fusion methods.

Table 2: Analysis of the performance of HEALNet in scenarios with missing modalities at inference, compared to uni-modal baselines. Each test sample contains only one of the two modalities. The HEALNet’s *hybrid early-fusion* generally achieves a higher average c-Index across all datasets.

Test set Dataset	50% Omic + 50% WSI		Omic + WSI
	Best Uni-modal	HEALNet	HEALNet
BLCA	0.547	0.612	0.668
BRCA	0.543	0.541	0.638
KIRP	0.644	0.714	0.812
UCEC	0.533	0.580	0.626

Specifically, using HEALNet trained with two modalities, we investigate its performance of missing modalities during inference. Note that, half of the test samples include only a WSI modality, while the other half only an omics modality, chosen randomly. The ‘Best Uni-Modal’ baseline corresponds to the uni-modal model’s prediction of the available modality in the same way that a late fusion model would use two uni-modal models followed by an XOR gating mechanism to make its prediction. The results from this analysis, given in Table 2, show that our proposed HEALNet, pre-trained on both modalities, archives stable and generally better performance than a late fusion baseline (as commonly performed in practice).

Discussion

In this work, we present HEALNet (**H**ybrid **E**arly-fusion **A**ttention **L**earning **N**etwork) – a flexible and scalable multi-modal approach for biomedical learning tasks. It is *hybrid* because it combines desirable properties of both early and intermediate fusion – the model is able to learn from the complete data, leveraging the shared latent space to capture cross-modal dependencies. We show that HEALNet outperforms both uni-modal and intermediate and late fusion multi-modal benchmarks. Specifically, HEALNet achieves state-of-the-art performance on four cancer survival prediction tasks (muscular bladder, breast, kidney, and endometrial cancer); both in terms of absolute performance as well as relative uplift from integrating multiple data modalities. Note that, while we evaluate HEALNet on two modalities, our approach can be readily extended to a larger number of modalities. HEALNet has several distinctive and beneficial properties that are useful for multi-modal

learning, in particular when applied in biomedical domains.

Structure-preserving fusion. The results support our hypothesis that HEALNet is able to learn the structural properties of each modality and convert the structural signal into better performance. The quantitative evidence of this is given by HEALNet’s absolute c-Index performance across tasks (Table 1), performing substantially better than the early fusion baseline that employs concatenation. Additionally, HEALNet allows for further qualitative analysis of this behaviour, as we can visualise the sample-level attention of different regions of the whole slide image. The attention maps in Figure 3 show a sample where the model identified multiple patches in the same region – distilling the wider image down to local information for which we would typically use convolutional networks.

HEALNet learns about high-level structural relationships by using a hybrid of modality-specific and shared parameters. For each modality, we learn attention weights (Equation 1) simultaneously in an end-to-end process. We believe that this distinguishes our hybrid early-fusion approach from conventional early and intermediate fusion methods. Instead of removing structural information (i.e., concatenation) or creating excessively large input tensors (i.e., Kronecker product), our hybrid early-fusion is able to preserve such structures by design. Similar to intermediate fusion methods, we use a shared latent space to capture cross-model dependencies. However, instead of creating a latent space through multiple encodings before combining them via a downstream function ($f(h_1, \dots, h_j; \phi)$), HEALNet learns an update function (Equation 3) that iteratively updates the shared latent with modality-specific information. Nevertheless, a limitation of such an approach is akin to training a higher number of parameters (i.e. large attention matrices), but on relatively few samples, making it prone to overfitting. Hence, we have found that HEALNet can be sensitive to the choice of regularisation mechanisms, even though the current regularisation techniques (such as L1 + SNN) have shown to be effective, as shown in Figure 4 (and extended in Appendix E).

Cross-modal learning. The motivation of using a hybrid-early fusion over a late fusion approach, is to enable the model to learn cross-modal interactions that are unavailable to modality-specific models trained in isolation. We can see the effect of this in Figure 2, showing HEALNet’s substantially higher uplift compared to the late fusion benchmark. We note, however, that using a multi-modal model is not

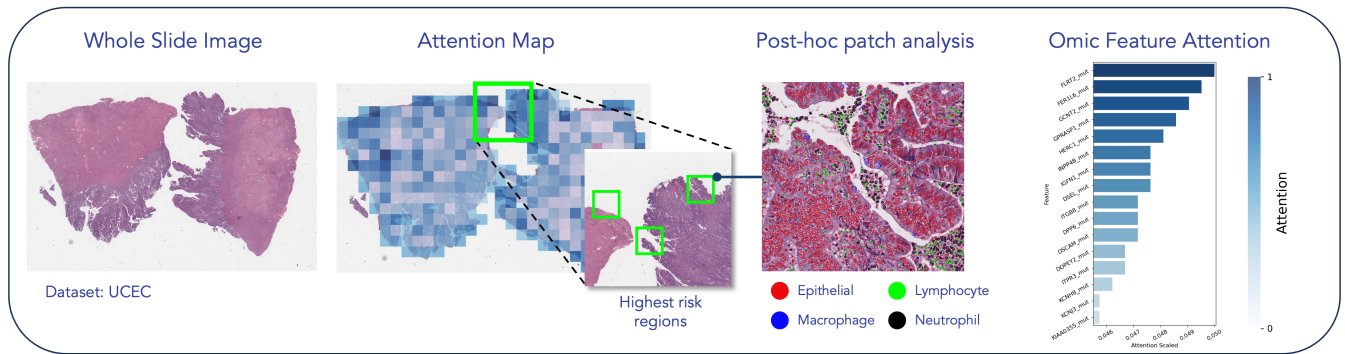


Figure 3: Illustration of model’s inspection capabilities using HEALNet on a high-risk patient of the UCEC study. We use the mean modality-specific attention weights across layers to highlight high-risk regions and inspect high-attention omic features. Individual patches can be used for further clinical or computational post-hoc analysis such as nucleus segmentation.



Figure 4: Effect of the regularisation mechanism. We show the train (top) and validation (bottom) losses on the KIRP dataset, of HEALNet variants with a) no regularisation (blue), b) only L1 regularisation (indigo), and c) L1 regularisation + a self-normalising network layer (green).

always a requirement, especially in the presence of *modality dominance* which we see on the UCEC dataset. However, HEALNet is robust to such cases, achieving comparable performance to the best uni-modal model. Upon further inspection of the HEALNet’s omic attention weights on the UCEC task, we found that they barely changed since their initialisation. As such, HEALNet was able to (correctly) inhibit this signal, which is not the case for the other multi-modal baselines where it leads to loss in performance.

Missing modality handling. Another key benefit of using iterative attention is that we can skip updates if modalities are missing at inference time without adding additional noise. For many intermediate fusion methods, missing modalities introduce noise since the fusion function $f()$ expects an intermediate representation h_m for all modalities. This requires initialising a random array or doing a latent search for a similar array to impute the missing portion. A practical approach to this challenge is a late fusion approach, which requires training and keeping several uni-modal alternatives, that can act as a substitution. This, however, can be computationally intensive. HEALNet, on the other hand,

overcomes this challenge by design. We believe that this underlines another key benefit of *hybrid early-fusion* – handling mixed missing modalities, at inference time, which takes advantage of multi-modal training, without introducing additional noise.

Inspections and explanations. Finally, another design benefit of using attention on the raw input data is that it allows for instance-level insights into the model’s behaviour, without the need for additional post-hoc explanation methods. Figure 3 shows what parts of the sample the model attends to on average across layers. For images, one can create a high-level heatmap of the cell tissue to highlight relevant regions for more detailed insights on the tumour microenvironment and disease progression. In turn, these regions can be further analysed in post-hoc, such as via nucleus segmentation. To showcase this capability, in Figure 3, we take the highest attention patches and perform nucleus segmentation into epithelial cells, lymphocytes, macrophages, and neutrophils using a HoverNet (Graham et al. 2019) pre-trained on the MoNuSAC dataset (Verma et al. 2021). We acknowledge that attention alone does not provide the entire view of the HEALNet’s behaviour, but nevertheless is a helpful capability for model inspection during development.

Conclusion

We introduce HEALNet, a flexible *hybrid early-fusion* approach for multi-modal learning. It has several distinctive and beneficial properties, suitable for applications in biomedical domains: 1) preserving structural signal of each modality through modality-specific attention, 2) learning cross-modal interactions due to its iterative architecture, 3) effective handling of missing modalities, and 4) easy model inspection. The experimental evaluation highlights the importance of fusing data early in the model pipeline to capture the cross-modal signal leading to better model performance, overall. While in this work we focus only on survival analysis using modalities from digital pathology and genomic data, we believe that our framework can also be extended to other domains (and modalities) such as radiology or precision oncology as well as other tasks such as diagnosis or predicting treatment response.

Acknowledgments

The authors would like to thank Philip Schouten for his insightful feedback. KH acknowledges support from the Gates Cambridge Trust via the Gates Cambridge Scholarship. NS acknowledges support from the Cancer Research UK Cambridge Centre [CTRQQR-2021/100012].

References

- Baltrusaitis, T.; Ahuja, C.; and Morency, L. P. 2019. Multimodal Machine Learning: A Survey and Taxonomy. *IEEE Transactions on Pattern Analysis and Machine Intelligence*, 41(2): 423–443. ArXiv: 1705.09406 Publisher: IEEE Computer Society.
- Bergstra, J.; Yamins, D.; and Cox, D. 2013. Making a Science of Model Search: Hyperparameter Optimization in Hundreds of Dimensions for Vision Architectures. In *Proceedings of the 30th International Conference on Machine Learning*, 115–123. PMLR. ISSN: 1938-7228.
- Brentnall, A. R.; and Cuzick, J. 2018. Use of the concordance index for predictors of censored survival data. *Statistical Methods in Medical Research*, 27(8): 2359–2373. Publisher: SAGE Publications Ltd STM.
- Cheerla, A.; and Gevaert, O. 2019. Deep learning with multimodal representation for pancreatic cancer prognosis prediction. *Bioinformatics*, 35(14): i446–i454.
- Chen, R. J.; Lu, M. Y.; Wang, J.; Williamson, D. F. K.; Rodig, S. J.; Lindeman, N. I.; and Mahmood, F. 2022a. Pathomic Fusion: An Integrated Framework for Fusing Histopathology and Genomic Features for Cancer Diagnosis and Prognosis. *IEEE Transactions on Medical Imaging*, 41(4): 757–770. Conference Name: IEEE Transactions on Medical Imaging.
- Chen, R. J.; Lu, M. Y.; Weng, W.-H.; Chen, T. Y.; Williamson, D. F.; Manz, T.; Shady, M.; and Mahmood, F. 2021. Multimodal Co-Attention Transformer for Survival Prediction in Gigapixel Whole Slide Images. In *2021 IEEE/CVF International Conference on Computer Vision (ICCV)*, 3995–4005. Montreal, QC, Canada: IEEE. ISBN 978-1-66542-812-5.
- Chen, R. J.; Lu, M. Y.; Williamson, D. F.; Chen, T. Y.; Lipkova, J.; Noor, Z.; Shaban, M.; Shady, M.; Williams, M.; Joo, B.; and Mahmood, F. 2022b. Pan-cancer integrative histology-genomic analysis via multimodal deep learning. *Cancer Cell*, 40(8): 865–878.e6. Publisher: Cell Press.
- Cui, C.; Yang, H.; Wang, Y.; Zhao, S.; Asad, Z.; Coburn, L. A.; Wilson, K. T.; Landman, B. A.; and Huo, Y. 2023. Deep multimodal fusion of image and non-image data in disease diagnosis and prognosis: a review. *Progress in Biomedical Engineering*, 5(2): 022001. Publisher: IOP Publishing.
- Dai, Y.; Gao, Y.; and Liu, F. 2021. TransMed: Transformers Advance Multi-Modal Medical Image Classification. *Diagnostics*, 11(8): 1384. Number: 8 Publisher: Multidisciplinary Digital Publishing Institute.
- Goyal, Y.; Mohapatra, A.; Parikh, D.; and Batra, D. 2016. Towards Transparent AI Systems: Interpreting Visual Question Answering Models. ArXiv:1608.08974 [cs].
- Graham, S.; Vu, Q. D.; Raza, S. E. A.; Azam, A.; Tsang, Y. W.; Kwak, J. T.; and Rajpoot, N. 2019. Hover-Net: Simultaneous segmentation and classification of nuclei in multi-tissue histology images. *Medical Image Analysis*, 58: 101563.
- Jaegle, A.; Gimeno, F.; Brock, A.; Zisserman, A.; Vinyals, O.; and Carreira, J. 2021. Perceiver: General Perception with Iterative Attention. *ICML*. ArXiv: 2103.03206.
- Klambauer, G.; Unterthiner, T.; Mayr, A.; and Hochreiter, S. 2017. Self-Normalizing Neural Networks. ArXiv:1706.02515 [cs, stat].
- Krizhevsky, A.; Sutskever, I.; and Hinton, G. E. 2012. ImageNet classification with deep convolutional neural networks. *Advances in neural information processing systems*, 25: 1097–1105.
- Liang, P. P.; Zadeh, A.; and Morency, L.-P. 2023. Foundations and Trends in Multimodal Machine Learning: Principles, Challenges, and Open Questions. ArXiv:2209.03430 [cs].
- Ma, F.; Laster, K.; and Dong, Z. 2022. The comparison of cancer gene mutation frequencies in Chinese and U.S. patient populations. *Nature Communications*, 13(1): 5651. Number: 1 Publisher: Nature Publishing Group.
- Sammut, S. J.; Crispin-Ortuzar, M.; Chin, S. F.; Provenzano, E.; Bardwell, H. A.; Ma, W.; Cope, W.; Dariush, A.; Dawson, S. J.; Abraham, J. E.; Dunn, J.; Hiller, L.; Thomas, J.; Cameron, D. A.; Bartlett, J. M.; Hayward, L.; Pharoah, P. D.; Markowitz, F.; Rueda, O. M.; Earl, H. M.; and Caldas, C. 2021. Multi-omic machine learning predictor of breast cancer therapy response. *Nature 2021 601:7894*, 601(7894): 623–629. Publisher: Nature Publishing Group.
- Steyaert, S.; Pizurica, M.; Nagaraj, D.; Khandelwal, P.; Hernandez-Boussard, T.; and Gevaert, O. 2023. Multimodal data fusion for cancer biomarker discovery with deep learning. *Nature Machine Intelligence*, 5(4): 351–362.
- Vaswani, A.; Brain, G.; Shazeer, N.; Parmar, N.; Uszkoreit, J.; Jones, L.; Gomez, A. N.; Kaiser, L.; and Polosukhin, I. 2017. Attention is All you Need. *Advances in Neural Information Processing Systems*, 30.
- Verma, R.; Kumar, N.; Patil, A.; Kurian, N. C.; Rane, S.; Graham, S.; Vu, Q. D.; Zwager, M.; Raza, S. E. A.; Rajpoot, N.; Wu, X.; Chen, H.; Huang, Y.; Wang, L.; Jung, H.; Brown, G. T.; Liu, Y.; Liu, S.; Jahromi, S. A. F.; Khani, A. A.; Montahaei, E.; Baghshah, M. S.; Behroozi, H.; Semkin, P.; Rassadin, A.; Dutande, P.; Lodaya, R.; Baid, U.; Baheti, B.; Talbar, S.; Mahbod, A.; Ecker, R.; Ellinger, I.; Luo, Z.; Dong, B.; Xu, Z.; Yao, Y.; Lv, S.; Feng, M.; Xu, K.; Zunnair, H.; Hamza, A. B.; Smiley, S.; Yin, T.-K.; Fang, Q.-R.; Srivastava, S.; Mahapatra, D.; Trnavska, L.; Zhang, H.; Narayanan, P. L.; Law, J.; Yuan, Y.; Tejomay, A.; Mitkari, A.; Koka, D.; Ramachandra, V.; Kini, L.; and Sethi, A. 2021. MoNuSAC2020: A Multi-Organ Nuclei Segmentation and Classification Challenge. *IEEE transactions on medical imaging*, 40(12): 3413–3423.
- Yu, J.; Li, J.; Yu, Z.; and Huang, Q. 2020. Multimodal Transformer With Multi-View Visual Representation for Image Captioning. *IEEE Transactions on Circuits and Systems for*

Video Technology, 30(12): 4467–4480. Conference Name: IEEE Transactions on Circuits and Systems for Video Technology.

Zadeh, S. G.; and Schmid, M. 2021. Bias in Cross-Entropy-Based Training of Deep Survival Networks. *IEEE Transactions on Pattern Analysis and Machine Intelligence*, 43(9): 3126–3137. Conference Name: IEEE Transactions on Pattern Analysis and Machine Intelligence.

A HEALNet Pseudocode

Algorithm 1: HEALNet

Input: Training data $X_m = \{x_1^{(1)}, \dots, x_j^{(n)}\}$; for modalities $m \in \{1, \dots, j\}$ and samples $N \in \{1, \dots, n\}$, where $m, N \in \mathbb{N}$.

Input: Survival training labels $Y = \{y^{(1)}, \dots, y^{(n)}\}$ for $S \in \{1, \dots, s\}$ survival bins, where $S, y^{(i)} \in \mathbb{N} \forall i = 1, \dots, n$.

Input: Number of fusion layers $d \in \mathbb{N}$.

Output: Logits of survival predictions $\hat{Y}_{logits} \in \{\hat{y}^{(1)}, \dots, \hat{y}^{(n)}\}$, where $\hat{y}^{(i)} \in \mathbb{R}, \forall i = 1, \dots, n$.

- 1: $S_0 \leftarrow \mathbb{R}^{c_l \times d_l}$ // S_0 is the latent array with $S_0[i, j] \sim \mathcal{U}(0, 1) \forall i \in \{1, \dots, c_l\}, j \in \{1, \dots, d_l\}$ for latent channels c_l and latent dimensions d_l .
 - 2: **for** fusion layer $l = 0, \dots, d - 1$ **do**
 - 3: $S_{l+j} \leftarrow FusionUpdate(S_l, X_m)$ // Equation 3
 - 4: **end for**
 - 5: $\hat{Y}_{logits} \leftarrow LinearHead(S_T)$ // where total timesteps $T = md \in \mathbb{N}$
 - 6: $\hat{Y}_{hazard} = sigmoid(\hat{Y}_{logits})$
 - 7: $Loss = NegativeLogLikelihood(Y, \hat{Y}_{hazard})$
 - 8: **return** \hat{Y}_{hazard}
-

Algorithm 2: Hybrid Early-fusion Layer (*FusionUpdate*)

Input: Latent array $S_t \in \mathbb{R}^{c_l \times d_l}$ at time step $t \in \{1, \dots, T\}$.

Input: Training data $X_m = \{x_1^{(1)}, \dots, x_j^{(n)}\}$ for modalities $m \in \{1, \dots, j\}$ and samples $N \in \{1, \dots, n\}$, where each $x_i^{(m)} \in \mathbb{R}^{d_x}$ and $m, N, d_x \in \mathbb{N}$. d_x corresponds to each modality's channel dimensions.

Output: $S_{t+j} \in \mathbb{R}^{c_l \times d_l}$.

- 1: **for** modality $m = 1, \dots, j$ **do**
 - 2: $Q_m \leftarrow W_m^{(q)} S_{t+m-1}$ where $W_m^{(q)} \in \mathbb{R}^{d_l}$ // query
 - 3: $K_m \leftarrow W_m^{(k)} X_m$ where $W_m^{(k)} \in \mathbb{R}^{d_x}$ // key
 - 4: $V_m \leftarrow W_m^{(v)} X_m$ where $W_m^{(v)} \in \mathbb{R}^{d_x}$ // value
 - 5: $\phi^{a_m} \leftarrow \{W_m^{(q)}, W_m^{(k)}, W_m^{(v)}\}$
 - 6: $a_m^{(t)} = \alpha(X_m, S_t; \phi^{a_m})$ // Attention, Equation 1
 - 7: $S_{t+m} = \psi(S_t, a_m^{(t)}; \rho)$ // Latent Update, Equation 2
 - 8: $S_{t+m} \leftarrow SNN(S_{t+m})$
 - 9: **end for**
 - 10: **return** S_{t+j}
-

B Experimental Results

While the main paper includes selected experimental results, where we only show the best uni-modal performance, the full list of experimental results can be found below.

Table 3: Full results of mean and standard deviation of the concordance Index on four survival risk categories. We trained HEALNet and all baselines on four The Cancer Genome Atlas (TCGA) tasks and report the performance on the hold-out test set across five cross-validation folds. A selection of these results are presented in Table 1.

Modalities	Model	BLCA	BRCA	KIRP	UCEC
Omic	Porpoise	0.590 ± 0.043	0.580 ± 0.027	0.780 ± 0.035	0.550 ± 0.026
	MCAT	0.552 ± 0.036	0.484 ± 0.045	0.721 ± 0.084	0.542 ± 0.065
	HEALNet (ours)	0.606 ± 0.019	0.456 ± 0.074	0.771 ± 0.135	0.439 ± 0.075
WSI	Porpoise	0.540 ± 0.030	0.550 ± 0.037	0.520 ± 0.037	0.630 ± 0.028
	MCAT	0.556 ± 0.039	0.489 ± 0.039	0.533 ± 0.099	0.602 ± 0.068
	HEALNet (ours)	0.487 ± 0.046	0.529 ± 0.042	0.518 ± 0.123	0.558 ± 0.072
Omic + WSI	Porpoise	0.620 ± 0.048	0.630 ± 0.040	0.790 ± 0.041	0.590 ± 0.034
	MCAT	0.620 ± 0.040	0.589 ± 0.073	0.789 ± 0.087	0.589 ± 0.062
	Early Fusion	0.565 ± 0.042	0.566 ± 0.068	0.783 ± 0.135	0.623 ± 0.107
	HEALNet (ours)	0.668 ± 0.036	0.638 ± 0.073	0.812 ± 0.055	0.626 ± 0.107

C Dataset Details

The results shown in this paper here are based upon data generated by the TCGA Research Network: <https://www.cancer.gov/tcga>. The Cancer Genome Atlas (TCGA) is an open-source genomics program run by the United State National Cancer Institute (NCI) and National Human Genome Research Institute, containing a total of 2.5 petabys of genomic, epigenomic, transcriptomic, and proteomic data. Over the years, this has been complemented by multiple other data sources such as the whole slide tissue images, which we use in this project. It contains data on 33 different cancer types for over 20,000 patients. Across the four cancer sites in the scope of this paper, we process a total of 2.5 Terabytes of imaging and omics data, the vast majority of which is taken up by the high-resolution whole slide images. Specifically, the four cancer sites are:

- Urothelial Bladder Carcinoma (BLCA): Most common type of bladder cancer, where the carcinoma starts in the urothelial cells lining the inside of the bladder.
- Breast Invasive Carcinoma (BRCA): Commonly referred to as invasive breast cancer refers to cancer cells that have spread beyond the ducts of lobules into surrounding breast tissue.
- Kidney Renal Papillary Cell Carcinoma (KIRP): Type of kidney cancer characterised by the growth of papillae within the tumour which is multi-focal, meaning that they frequently occur in more than one location in the kidney.
- Uterine Corpus Endometrial Carcinoma (UCEC): Most common type of uterine cancer arising in the endometrium, i.e., the lining of the uterus.

Table 4: Overview of data availability and dimensionality of the four TCGA datasets used for experiments.

Property	BLCA	BRCA	KIRP	UCEC
Slide samples	436	1,019	297	566
Omic samples	437	1,022	284	538
Overlap (n used)	436	1,019	284	538
Omic features used	2,191	2,922	1,587	1,421
WSI resolution (px)	79,968 x 79,653	35,855 x 34,985	72,945 x 53,994	105,672 x 71,818
Censorship share	53.9%	86.8%	84.5%	85.5%
Survival bin sizes	[72, 83, 109, 172]	[403, 289, 172, 155]	[43, 56, 113, 72]	[68, 143, 83, 244]
Disk space (GB)	594	883	275	756

D Hyperparameters

Table 5: Overview of Hyperparameters used in the final code implementation. Parameters that are consistent across datasets can be set in the `config/main_gpu.yml` and dataset-specific parameters can be set in `config/best_hyperparameters.yml`

Scope	Paramter	BLCA	BRCA	KIRP	UCEC
<i>Shared</i>	Output dims	4	4	4	4
	Patch Size	256	256	256	256
	Loss	NLL	NLL	NLL	NLL
	Loss weighting	inverse	inverse	inverse	inverse
	Subset	uncensored	uncensored	uncensored	uncensored
	Batch Size	8	8	8	8
	Epochs	50	50	50	50
	Early stopping patience	5	5	5	5
	Scheduler	OneCycle LR	OneCycle LR	OneCycle LR	OneCycle LR
	Max LR	0.008	0.008	0.008	0.008
	Momentum	0.92	0.92	0.92	0.92
	Optimizer	Adam	Adam	Adam	Adam
	L1 reg	0.00001	0.000006	0.00004	0.0003
<i>HEALNet</i>	Layers	2	2	5	2
	Shared Array dims	25 x 119	17 x 126	17 x 62	16 x 65
	Attention heads	8	8	8	8
	Dims per head	16	63	27	103
	Attention dropout	0.08	0.46	0.32	0.25
	Feedforward dropout	0.47	0.36	0.05	0.06

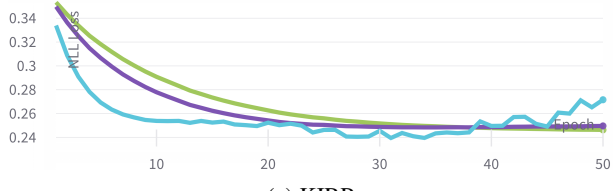
E Regularisation mechanisms



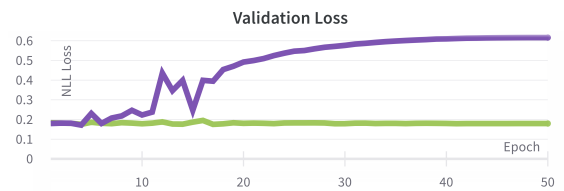
(a) BLCA



(b) BRCA



(c) KIRP



(d) UCEC

Figure 5: Effect of the regularisation mechanism. We show the train (top) and validation (bottom) losses on all tested datasets, of HEALNet variants with a) no regularisation (blue), b) only L1 regularisation (indigo), and c) L1 regularisation + a self-normalising network layer (green).